5292 *Chem. Mater.* **2009,** *21,* 5292–5299
DOI:10.1021/cm902404s

CHEMISTRY OF MATERIALS
Article

# Hybrid Core−Shell Nanoparticles: Photoinduced Electron-Transfer for Charge Separation and Solar Cell Applications

Asim Guchhait, Arup K. Rath, and Amlan J. Pal*

*Department of Solid State Physics, Indian Association for the Cultivation of Science, Jadavpur, Kolkata 700032, India*

*Received August 5, 2009. Revised Manuscript Received September 24, 2009*

We report growth and formation of hybrid core−shell nanoparticle systems, where photoinduced electron-transfer takes place from the II−VI semiconducting core to an organic shell. With the hybrid core−shell nanoparticles, we fabricate devices so that the photoinduced electron-transfer can finally yield photocurrent and result photovoltaic solar cells. Formation of an organic shell-layer on CdSe nanoparticles is supported by electronic absorption spectroscopy. Electron-transfer from the nanoparticle in the core to a number of organic molecules in the shell is established from quenching of photoluminescence intensity of CdSe nanoparticles as well as from a change in the lifetime of photoluminescence emission. Devices based on the hybrid core−shell nanoparticles in a suitable hole-transporting layer with two dissimilar metal electrodes show efficient photovoltaic performance. Here, following the electron-transfer, electrons flow through the organic molecules and holes, left in the nanoparticles, move through the hole-transporting polymer to the opposite electrodes to yield photovoltaic short-circuit current. The role of CdSe nanoparticles in light-harvesting and charge-generation has been substantiated by control experiments with ZnS nanoparticles in the core. In ZnS-based hybrid core−shell systems, photovoltaic performance is low since photoinduced electron-transfer does not occur from ZnS to the dye.

## 1. Introduction

In organic or polymeric solar cells, device operation involves (1) exciton generation, (2) charge separation, and (3) carrier transport to the opposite electrodes.[1−6] Since the three steps occur in sequence, efforts have been made to enhance efficiency or output of each of the steps. Generation of excitons expectedly depends on matching of electronic absorption spectrum of the active material with that of the solar illumination. Hence active materials are chosen accordingly. Exciton dissociation or charge separation, which occurs at the interface between a donor and an acceptor layer, takes place due to the internal field that develops owing to the difference of energy levels at the interfaces. Carrier transport, the third step, is directed by the internal field generated by the difference in workfunctions of the two electrodes. Apart from the electric-field, mobility of charge carriers plays a major role in determining the short-circuit current of photovoltaic devices.

Considering the limitation of organic and polymeric materials in each of the steps of device operation, efforts have been made to incorporate nanoparticles and nanowires in photovoltaic devices.[7−21] In this regard, II−VI semiconducting nanoparticles, having the ability to

*Corresponding author. E-mail: sspajp@iacs.res.in.

(1) Yu, G.; Gao, J.; Hummelen, J. C.; Wudl, F.; Heeger, A. J. *Science* **1995**, *270*, 1789.
(2) Halls, J. J. M.; Walsh, C. A.; Greenham, N. C.; Marseglia, E. A.; Friend, R. H.; Moratti, S. C.; Holmes, A. B. *Nature* **1995**, *376*, 498.
(3) Chen, L. C.; Godovsky, D.; Inganas, O.; Hummelen, J. C.; Janssens, R. A. J.; Svensson, M.; Andersson, M. R. *Adv. Mater.* **2000**, *12*, 1367.
(4) Brabec, C. J.; Cravino, A.; Zerza, G.; Sariciftci, N. S.; Kiebooms, R.; Vanderzande, D.; Hummelen, J. C. *J. Phys. Chem. B* **2001**, *105*, 1528.
(5) Peumans, P.; Yakimov, A.; Forrest, S. R. *J. Appl. Phys.* **2003**, *93*, 3693.
(6) Vanlaeke, P.; Swinnen, A.; Haeldermans, I.; Vanhoyland, G.; Aernouts, T.; Cheyns, D.; Deibel, C.; D'Haen, J.; Heremans, P.; Poortmans, J.; Manca, J. V. *Sol. Energy Mater. Sol. Cells* **2006**, *90*, 2150.
(7) Mattoussi, H.; Rubner, M. F.; Zhou, F.; Kumar, J.; Tripathy, S. K.; Chiang, L. Y. *Appl. Phys. Lett.* **2000**, *77*, 1540.
(8) Ruani, G.; Fontanini, C.; Murgia, M.; Taliani, C. *J. Chem. Phys.* **2002**, *116*, 1713.
(9) Kim, Y. G.; Walker, J.; Samuelson, L. A.; Kumar, J. *Nano Lett.* **2003**, *3*, 523.
(10) Tokuhisa, H.; Hammond, P. T. *Adv. Funct. Mater.* **2003**, *13*, 831.
(11) Huynh, W. U.; Dittmer, J. J.; Libby, W. C.; Whiting, G. L.; Alivisatos, A. P. *Adv. Funct. Mater.* **2003**, *13*, 73.
(12) Bhattacharyya, S.; Kymakis, E.; Amaratunga, G. A. J. *Chem. Mater.* **2004**, *16*, 4819.
(13) Gur, I.; Fromer, N. A.; Geier, M. L.; Alivisatos, A. P. *Science* **2005**, *310*, 462.
(14) Pradhan, B.; Batabyal, S. K.; Pal, A. J. *Appl. Phys. Lett.* **2006**, *88*, 093106.
(15) Sun, B. Q.; Greenham, N. C. *Phys. Chem. Chem. Phys.* **2006**, *8*, 3557.
(16) Kim, J. Y.; Lee, K.; Coates, N. E.; Moses, D.; Nguyen, T. Q.; Dante, M.; Heeger, A. J. *Science* **2007**, *317*, 222.
(17) Nogueira, A. F.; Lomba, B. S.; Soto-Oviedo, M. A.; Correia, C. R. D.; Corio, P.; Furtado, C. A.; Hummelgen, I. A. *J. Phys. Chem. C* **2007**, *111*, 18431.
(18) Saunders, B. R.; Turner, M. L. *Adv. Colloid Interface Sci.* **2008**, *138*, 1.
(19) Kongkanand, A.; Tvrdy, K.; Takechi, K.; Kuno, M.; Kamat, P. V. *J. Am. Chem. Soc.* **2008**, *130*, 4007.
(20) Goodman, M. D.; Xu, J.; Wang, J.; Lin, Z. Q. *Chem. Mater.* **2009**, *21*, 934.
(21) Zotti, G.; Vercelli, B.; Berlin, A.; Chin, P. T. K.; Giovanella, U. *Chem. Mater.* **2009**, *21*, 2258.


Published on Web 10/13/2009

photogenerate multiple excitons,[22−24] are promising materials for solar cell application. The (insulating) stabilizing agents do however pose some problems. While the inert stabilizers forbid formation of an efficient interface between nanoparticles and a hole-transporting polymer, removal of the stabilizing agents makes the polymer: nanoparticle films inhomogeneous due to immiscibility of the components in a common solvent; still, with the removal of the stabilizing agent, the external quantum efficiency (EQE) increased from 25 to 59%.[11] Use of hybrid core−shell nanoparticles with suitable organic molecules in the shell may be a route to improve the interface.

Since nanoparticles' ability in the first and third steps of a (photovoltaic) device, namely, exciton generation and carrier transport, is already established, the onus is on the second step (i.e., charge separation) to favorably use nanoparticles in photovoltaic devices. Photoinduced electron-transfer from a semiconducting quantum dot to another quantum dot[25] or to certain organic molecules has been reported to be an ultrafast one.[26−28] We aimed to take advantage of this ultrafast electron-transfer process in photovoltaic devices. That is, our target is to make use of the electron-transfer process so that there can be transports of electrons that have been transferred to the organic molecules and holes that are left in the nanoparticles to the opposite direction or electrodes. In this way, we aim to convert the ultrafast photoinduced electron-transfer process into short-circuit current in the external circuit for efficient hybrid photovoltaic solar-cell application. Here, we choose the shell molecules in such a way that they form a homogeneous interface with the host polymer.

## 2. Experimental Section

**Formation of Hybrid Core−Shell Nanoparticles.** CdSe nanoparticles were synthesized following standard methods.[29,30] In brief, 0.256 g (2.0 mmol) of CdO, 5.649 g (20 mmol) oleic acid, and 9 mL 1-octadecene were mixed in a 50 mL three-neck flask and heated to 275 °C under continuous flow of nitrogen. When CdO was dissolved completely, the solution was allowed to cool down to room temperature. A 3 g portion each of trioctylphosphine oxide (TOPO) and octadecylamine (ODA) were then added to the solution. The mixture was further heated to 300 °C under nitrogen environment. A 3 mL portion of selenium stock solution (prepared by dissolving 1.8 g of Se in 8.5 mL of tributyl phosphate and sonicating to dissolve completely) was then swiftly injected to the flask. The solution was then rapidly cooled down to 70 °C. The CdSe nanoparticles were extracted by repeated precipitation in chloroform/acetone followed by centrifuge at 8000 rpm. Excess TOPO and ODA were removed by precipitation in methanol. The resulting nanocrystals were redispersed in chloroform for further use. CdSe nanoparticles had an average diameter of 2.5 nm (as obtained from high-resolution transmission electron microscopy images and also supported by the value calculated from peak wavelength of electronic absorption spectroscopy).

As acceptor molecules, Rose Bengal (RB), Phloxine B (PB), and sodium salt of Tetrabromophenol Blue (TBrPh) were chosen. These molecules have several halogens as functional groups that make them electron-accepting in nature. In addition, the molecules have at least one −COONa group (or a $-SO_3Na$ group) that allows amide linkage with the $-NH_2$ moiety of the stabilizer upon annealing.[31,32] In practice, water solution of a dye (0.3 mL, 1 mM) was added to the dispersed solution of the nanoparticle in chloroform. As expected, the two solutions remained separated with the dye solution remaining on top. With time, amide linkage between the dye molecule and the stabilizer formed yielding hybrid core−shell nanoparticles. By recording electronic absorption spectroscopy of the lower section of the column at different time intervals, adsorption of dye molecules with the nanoparticles was monitored. Extent of dye adsorption on CdSe nanoparticles has been measured (by Beer's law) from extinction coefficients of the individual components. From the extinction coefficient of RB ($\varepsilon$ = 90 400 at 564 nm) and CdSe ($\varepsilon$ = 71 596 at 524 nm),[33] molar concentration of RB as compared to that of CdSe (in %) in the core−shell solution has been determined and specified to denote a particular CdSe:RB core−shell nanoparticle. For control experiments with ZnS:dye core−shell hybrid nanoparticles, ZnS nanoparticles were synthesized from zinc stearate and sulfur powder in ODE solution and in presence of ODA; the procedure of dye adsorption on ZnS nanoparticles remained the same.

**Studies of Photoinduced Electron-Transfer.** Photoluminescence (PL) spectroscopy of the nanoparticles with different degree of dye-adsorption has been recorded with a Spex Fluoromax 4P emission spectrophotometer. While keeping the excitation wavelength the same, PL spectra were recorded at different times or different stages of dye-adsorption. Exciton lifetime of PL intensity has been recorded with a time-correlated single photon counting (TCSPC) spectrometer, Horiba Jobin Yvon Fluorohub.

**Device Fabrication.** Devices were fabricated on indium tin oxide (ITO) coated glass substrates. The ITO substrates had a surface resistance of 15 Ω/sq. A 30 nm-thick layer of PEDOT:PSS (Baytron P 4083) was first spun on stripped ITO substrates. The films were annealed at 150 °C for 15 min to obtain a highly conductive layer that maintained a low series resistance. On top of the PEDOT:PSS film, an active layer for photovoltaic devices was spun from a mixed solution of poly(3-hexylthiophene) (P3HT) and hybrid core−shell nanoparticles. The weight ratio between P3HT and core−shell nanoparticles in the spinning solution was varied. Selected P3HT:nanoparticle ratios were 2:1, 1:1, 1:2, 1:3, and 1:4. In one of the cases, P3HT:nanoparticle ratio being 1:1, the content of the dye molecules on the nanoparticles varied between 10% and 40%. As control devices

(22) Schaller, R. D.; Agranovich, V. M.; Klimov, V. I. *Nat. Phys.* **2005**, *1*, 189.
(23) Shabaev, A.; Efros, A. L.; Nozik, A. J. *Nano Lett.* **2006**, *6*, 2856.
(24) Schaller, R. D.; Sykora, M.; Pietryga, J. M.; Klimov, V. I. *Nano Lett.* **2006**, *6*, 424.
(25) Tu, H. H.; Kelley, D. F. *Nano Lett.* **2006**, *6*, 116.
(26) Boulesbaa, A.; Issac, A.; Stockwell, D.; Huang, Z.; Huang, J.; Guo, J.; Lian, T. *J. Am. Chem. Soc.* **2007**, *129*, 15132.
(27) Huang, J.; Stockwell, D.; Huang, Z. Q.; Mohler, D. L.; Lian, T. Q. *J. Am. Chem. Soc.* **2008**, *130*, 5632.
(28) Issac, A.; Jin, S. Y.; Lian, T. Q. *J. Am. Chem. Soc.* **2008**, *130*, 11280.
(29) Qu, L. H.; Peng, X. G. *J. Am. Chem. Soc.* **2002**, *124*, 2049.
(30) Swafford, L. A.; Weigand, L. A.; Bowers, M. J.; McBride, J. R.; Rapaport, J. L.; Watt, T. L.; Dixit, S. K.; Feldman, L. C.; Rosenthal, S. J. *J. Am. Chem. Soc.* **2006**, *128*, 12299.
(31) Harris, J. J.; DeRose, P. M.; Bruening, M. L. *J. Am. Chem. Soc.* **1999**, *121*, 1978.
(32) Mendelsohn, J. D.; Barrett, C. J.; Chan, V. V.; Pal, A. J.; Mayes, A. M.; Rubner, M. F. *Langmuir* **2000**, *16*, 5017.
(33) Yu, W. W.; Qu, L. H.; Guo, W. Z.; Peng, X. G. *Chem. Mater.* **2003**, *15*, 2854.

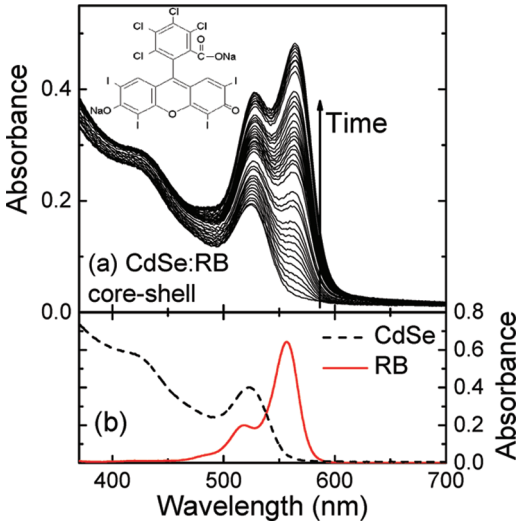


**Figure 1.** Electronic absorption spectra of (a) CdSe:RB core−shell and (b) CdSe nanoparticles in dispersed solution in chloroform and RB solution in methanol. In part a, spectra at different times after addition of RB solution in CdSe dispersed solution from the top are shown. Duration of time ranged from 0 to 120 min, as marked by an arrow. The structural formula of RB is shown in part a.

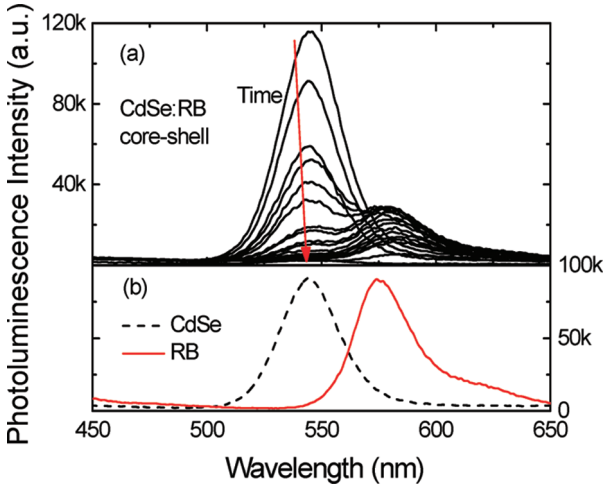


**Figure 2.** Photoluminescence spectra of (a) CdSe:RB core−shell and (b) CdSe nanoparticles in dispersed solution in chloroform and RB solution in methanol. In part a, spectra at different times after addition of RB solution in CdSe dispersed solution from the top are shown. The duration of time ranged from 0 to 30 min, as marked by an arrow. The excitation wavelength for all the spectra was 375 nm.

without any dye molecules, films with only the nanoparticles in P3HT were also spun. The thickness of the active layer ranged between 180 and 220 nm. To complete device fabrication, orthogonal strips of aluminum electrodes (100 nm) were thermally evaporated in vacuum ($\sim 10^{-6}$ Torr). The area of the devices was 4 $mm^2$.

**Device Characterization.** For electrical characterization, devices were kept in a shielded vacuum chamber. Current−voltage ($I-V$) characteristics under dark and different illumination conditions were recorded with a Keithley 6517A Electrometer. Bias was applied to the ITO electrode with respect to the Al one. A 150 W Newport-Stratfort Solar Simulator model 76500, attached with an AM 1.5 filter, acted as the source for illumination. The intensity of the simulated solar illumination was varied between 10 and 100 $mW/cm^2$ with neutral density filters.

## 3. Results and Discussion

**Electronic Absorption Spectroscopy: Formation of Hybrid Core−Shell Nanoparticles.** We formed core−shell nanoparticles with CdSe particles in the core and different dye molecules in the shell. While ODA-capped CdSe nanoparticles were dispersed in chloroform, the dyes were dissolved in water. By adding a dye solution to the dispersed solution of CdSe, the mixture remained separable with the dye solution on top. Electronic absorption spectra of the lower portion of the column were recorded as a function of time. Results at different extents of RB adsorption are shown in Figure 1a. For comparison, absorption spectra of the components are shown in Figure 1b. Electronic absorption spectra of hybrid core−shell nanoparticles with other dye molecules at different extents of dye adsorption, along with that of their components, are shown in the Supporting Information (Figures S1 and S2). Upon comparison, we can infer from Figure 1 that initially the spectrum shows bands related to only the CdSe nanoparticles (at 528 nm). With time, the band corresponding to RB started to appear in the longer wavelength region (564 nm). The band due to RB grew with time, increased beyond that of CdSe, and finally reached saturation. The intensity of the band due to CdSe nanoparticles expectedly remained the same (if one subtracts the short-wavelength component of RB absorption intensity). Growth of the RB-band indicates that with time the dye molecules came in the vicinity of CdSe nanoparticles in the dispersed solution. In control experiments without any nanoparticles in chloroform and upon addition of RB solution on top, the RB-band did not appear in the absorption spectrum of the lower section of the column. The results hence show that RB molecules have become adsorbed to CdSe nanoparticles and formed hybrid core−shell nanoparticles (as also supported by PL measurements). Had the molecules only entered the CdSe dispersed solution without any linkage with the nanoparticles, they would have done so even in the control experiment (in absence of CdSe nanoparticles). The capping of the nanoparticles hence played a major role in the adsorption of RB molecules on CdSe nanoparticles. The linkage between the ODA-cappings of nanoparticles ($-NH_2$ moieties) and RB molecules with $-COONa$ groups can be expected to be amide in nature.

**Photoluminescence Spectroscopy: Photoinduced Electron-Transfer.** That the organic dye molecules actually linked to the nanoparticles can be established from PL measurements. After adding the dye solution in a dilute CdSe dispersed solution from top, we recorded the PL spectrum of the lower section of the column. The PL spectra for the CdSe:RB core−shell system at different times are presented in Figure 2a. Initially, the spectrum shows a band at 545 nm that corresponds to that of CdSe nanoparticles. As time increases, PL intensity corresponding to CdSe nanoparticles quenches; a new shoulder (and then a band) appears at 580 nm that corresponds to PL emission of RB; with time, the PL of RB decreases. Finally, the PL of CdSe is totally quenched

leaving very little PL characteristics of only the RB molecules. The analysis is supported by PL emission of the components, that is, by the PL emission of CdSe nanoparticles in dispersed solution and RB solutions, as presented in Figure 2b. From the PL spectra of core−shell nanoparticles at different extents of dye adsorption, photophysical processes, such as energy transfer[34] and electron-transfer, which occur following photon absorption, can be understood. Since the excitation wavelength was within the excitation spectrum of the dye, the initial rise in PL at 580 nm could be due to the free dye molecules in the solution before they were attached to CdSe. Once the molecules become attached to the quantum dots, they stop to yield PL due to photoinduced electron-transfer from the dots. With an electron-transfer, the extra electron goes to the ground state of the dye molecule and creates a radical anion. Due to the presence of this extra charge, a direct excitation produced in Rose Bengal interacts with this charge and recombines through a nonradiative path leading to quenching of PL at 580 nm. PL quenching in systems with other dye molecules is presented in the Supporting Information (Figures S3 and S4).

The quenching of CdSe emission is due to adsorption of the dye molecules on the nanoparticles. PL quenching upon linkage of RB molecules suggests that a photoinduced electron-transfer has occurred from CdSe nanoparticles to the dye molecules. This has become possible due to the electron-accepting nature or low reduction potential of the molecules. Upon addition of a dye solution to CdSe dispersed solution from the top, the solutions remained separated since they were immiscible. With time, RB molecules become adsorbed to the nanoparticles through amide linkage. In such CdSe:RB core−shell systems, photoinduced electron-transfer from the nanoparticles to the dye molecules leads to PL quenching of CdSe emission. A continuous decrease in the PL intensity of CdSe nanoparticles with time implies that the dye molecules always become attached or linked to the nanoparticles itself, forming hybrid core−shell nanoparticles with CdSe in the core and a monolayer of dye molecules as a shell.

Linkage of RB molecules and correspondingly photoinduced electron-transfer from the nanoparticles to the dye molecules are further supported by lifetime measurements. Decay dynamics of CdSe nanoparticles without and with RB linkage of different degrees or levels are shown in Figure 3. Average lifetimes of different systems have been tabulated in the figure. For the CdSe nanoparticles, the lifetime (23.3 ns) matches well with the reported value; the correspondence between the change in lifetime and content of adsorbed molecules also matches with the reported behavior.[28] The results show that exciton lifetime of CdSe nanoparticles decreased by more than 1 order of magnitude due to RB linkage. With an increase in the concentration of RB on the shell of CdSe nanoparticles, the PL decay process becomes fast.

(34) Lutich, A. A.; Jiang, G.; Susha, A. S.; Rogach, A. L.; Stefani, F. D.; Feldmann, J. *Nano Lett.* **2009**, *9*, 2636.

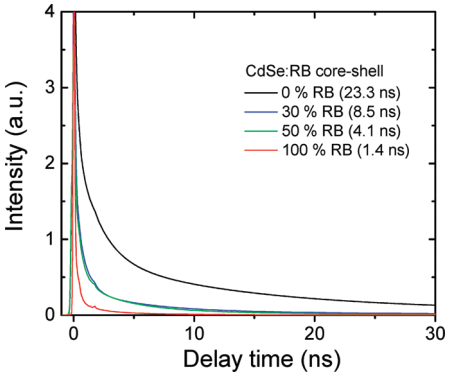


**Figure 3.** Fluorescence decay profile of the PL emission of CdSe and CdSe with different amount of RB molecules (CdSe:RB core−shells). Exciton lifetimes of the systems are shown in the parentheses of the legends. Excitation wavelength for all the decays was 375 nm.

(Measurement could not be carried out with a still lower extent of RB adsorption on CdSe nanoparticles.) In the core−shell system, the decay-profile contains a long-lifetime component, which could be due to the nanoparticles that were left unperturbed. The decrease in the exciton lifetime of CdSe nanoparticles confirms ultrafast electron-transfer from CdSe nanoparticle to RB molecules. The results hence show that upon photoillumination, electron-transfer occurs in CdSe:RB hybrid core−shell nanoparticles.

**Photovoltaic Devices: Exciton Dissociation through Electron-Transfer.** Photoinduced electron-transfer from CdSe nanoparticles to RB molecules implies that excitons generated in CdSe have been dissociated. Since exciton dissociation is a primary criterion for a photovoltaic device, we aimed to use these hybrid core−shell nanoparticles in solar cells. These core−shell nanoparticles offer unique advantage that almost all the photogenerated excitons can be dissociated via electron-transfer. (In conventional donor/acceptor-type photovoltaic cells, excitons generated only near an interface become dissociated; other excitons, generated apart by a distance of exciton diffusion length, decay in a radiative or in a nonradiative way; dissociation of excitons at the donor/acceptor interfaces is followed by movement of holes and electrons through the hole-transporting donor and the electron-transporting acceptor layer, respectively.) Hence, to extract the electrons and holes toward opposite directions, we introduced the core−shell nanoparticles in a hole-transporting layer (P3HT) that also acted as a matrix and sandwiched the layer between two electrodes of dissimilar workfunctions (ITO and Al). $I-V$ characteristics of the devices under dark conditions are expectedly rectifying in nature. Characteristics of an ITO/PEDOT:PSS/P3HT:(CdSe:RB)/Al device in the dark and under 100 mW/cm$^2$ illumination conditions are shown in Figure 4a. Under illumination, the $I-V$ characteristics show photovoltaic behavior with a short-circuit current ($I_{SC}$) of 0.65 mA/cm$^2$, an open-circuit voltage ($V_{OC}$) of 0.57 V, a fill-factor (FF) of 0.32, and a power conversion efficiency ($\eta$) of 0.12%. (With 470 nm as the illumination wavelength and an intensity of

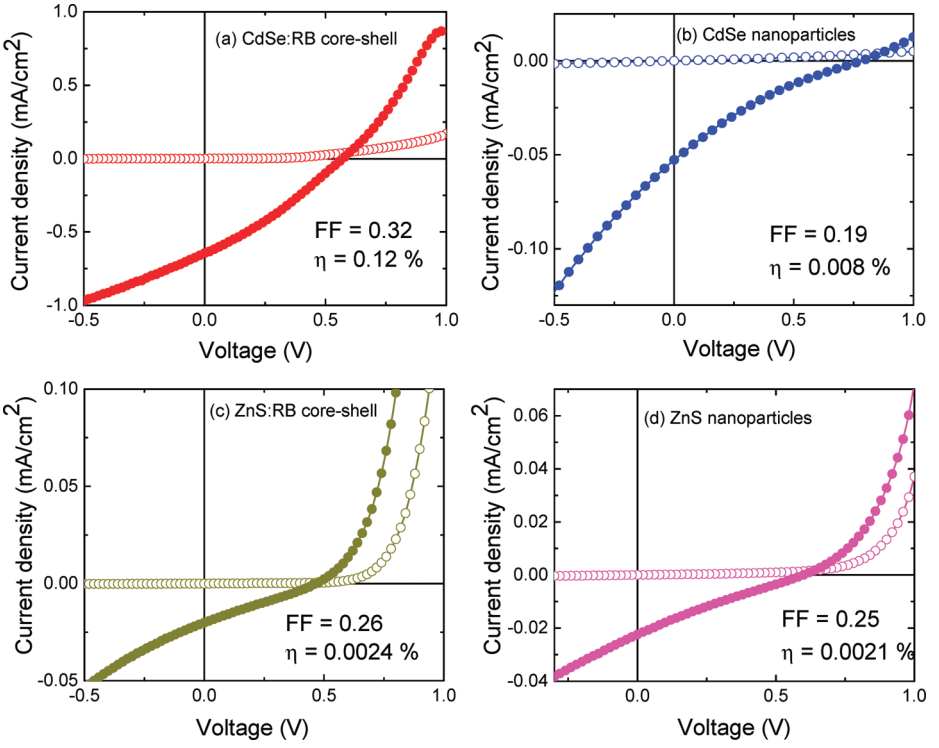


**Figure 4.** $I-V$ characteristics of devices based on CdSe and ZnS nanoparticles with and without RB molecules on the shell, namely (a) ITO/PEDOT:PSS/**P3HT:(CdSe:RB)**/Al, (b) ITO/PEDOT:PSS/**P3HT:CdSe**/Al, (c) ITO/PEDOT:PSS/**P3HT:(ZnS:RB)**/Al, and (d) ITO/PEDOT:PSS/**P3HT:ZnS**/Al devices under dark (open symbols) and 100 mW/cm$^2$ illumination (filled symbols) conditions. Fill-factor (FF) and power conversion efficiency ($\eta$) of the devices are quoted in the respective figures.

1.18 mW/cm$^2$, $\eta$ of the device rises to 1.36%). In these devices, excitons generated at CdSe nanoparticles dissociate due to electron-transfer to RB molecules on the shell. As each of the nanoparticles is surrounded by a number of RB molecules, multiple excitons generated in these II−VI quantum dots could dissociate in the CdSe:RB core−shell system. The electric field due to dissimilar workfunctions of the two electrodes drives the holes left in CdSe nanoparticles through the hole-transporting P3HT layer toward PEDOT:PSS and ITO electrode; electrons in RB molecules are similarly driven toward the Al electrode. A short-circuit current is hence observed in the external circuit. As the RB molecules are in the outer surface of the nanoparticles, P3HT would make a homogeneous interface with the core−shell nanoparticles; the P3HT/RB interfaces can also dissociate excitons, which are photogenerated in P3HT. With another dye in the shell of core−shell hybrid nanoparticles, where photoinduced electron-transfer from the nanoparticle to the dye occurs, characteristics of a similar device in dark and under 100 mW/cm$^2$ illumination conditions are shown in the Supporting Information (Figure S5a).

**Control Experiment I (a System without the Dye).** That a photoinduced electron-transfer is the key process in the observed photovoltaic behavior can be verified by studying a similar system where electron-transfer from CdSe nanoparticles is not possible. We fabricated a device without RB molecules on CdSe nanoparticles, namely the ITO/PEDOT:PSS/P3HT:CdSe/Al structure. $I-V$ characteristics of the device in the dark and the same illumination condition are shown in Figure 4b. In the absence of RB molecules, $I-V$ characteristics in dark conditions have a lower rectification ratio than that with RB molecules in the shell. This is due to lowering of the electron injecting barrier in the latter system. Photovoltaic properties of the device based on CdSe nanoparticles without any RB molecules drop sharply. $I_{SC}$ and $\eta$ are lower by more than 1 order of magnitude than the system with RB molecules. A comparison of the plots in Figure 4a and b shows that FF is also low in the system without RB. There is some enhancement of $V_{OC}$ in the latter system though. The origin of the little photovoltaic activity and $I_{SC}$ in the P3HT:CdSe bulk-heterojunction system could be due to exciton dissociation at the P3HT/CdSe interfaces. In such a system upon photoillumination, while P3HT acts as the hole-transporting layer, the electrons might have hopped through the CdSe nanoparticles, which are, in fact, *n*-type semiconductors, to reach the Al electrode. As compared to a fast and efficient electron-transfer process in CdSe:RB hybrid core−shells, the P3HT/CdSe interfaces are weak in exciton dissociation; photovoltaic response in this system has hence remained low (Figure 4b).

**Control Experiment II (a System with ZnS:RB).** The evidence of CdSe participation in light-harvesting and charge-generation processes has been substantiated by experiments with a control system with ZnS nanoparticles. ZnS nanoparticles have a substantially high excited-state reduction potential as compared to CdSe;[28,35] electron-transfer from ZnS to a dye is hence expected to be a

(35) Zeug, N.; Bucheler, J.; Kisch, H. *J. Am. Chem. Soc.* **1985**, *107*, 1459.

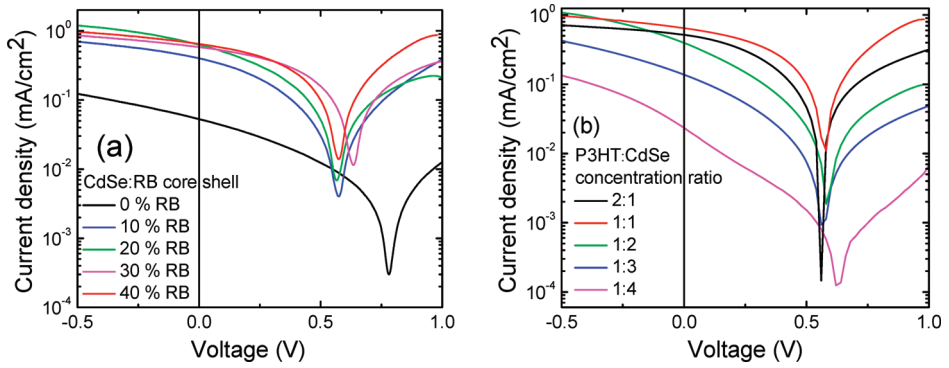


**Figure 5.** Current−voltage characteristics in a log−linear scale of the ITO/PEDOT:PSS/P3HT:(CdSe:RB)/Al device with (a) varied RB concentration and (b) different content of core−shell nanoparticles in P3HT.

slow process or energetically not favorable. We have studied electronic absorption spectroscopy of ZnS:RB core−shell systems at different extents of dye adsorption. While electronic absorption spectra evidence adsorption of the dye to form hybrid core−shell nanoparticles (ZnS:RB), PL intensity corresponding to ZnS nanoparticles did not show any quenching (parts a and b of Figure S6, respectively). Neither was there any change in the exciton lifetime of ZnS nanoparticles upon RB linkage (Figure S7). Both the results show that there was no electron-transfer from ZnS to RB.

We have fabricated devices with the ZnS:RB core−shell nanoparticles and characterized them; we also fabricated a device without RB molecules on ZnS nanoparticles (in P3HT matrix). Results based on ZnS nanoparticles with and without RB are presented in Figure 4c and d, respectively. In each of the figures, $I-V$ characteristics under dark and illumination conditions are shown. The figures show that with the addition of RB on the shell of ZnS, $I_{SC}$ does not improve. This is due to absence of photoinduced electron-transfer in the ZnS:RB system. The results with ZnS are in contrast to that with CdSe nanoparticles where $I_{SC}$ increased by 1 order of magnitude due to addition of RB in the shell. The results hence show the importance of photoinduced electron-transfer in CdSe:RB systems in resulting photocurrent.

It is intriguing to compare results from devices based on CdSe:RB and ZnS:RB core−shells. Since all other parameters of these devices shown in Figure 4a and c, respectively, are identical, we could compare photovoltaic performance of the two devices. $I_{SC}$ in the latter device is 30 times lower than that of the CdSe:RB-based system. Since the content of RB has remained the same in both the systems, the results, in conjunction with absence of electron-transfer from ZnS to RB, show the participation of CdSe nanoparticles in light-harvesting and charge-generation processes. Had the nanoparticles been acted only as physical scaffolds for organizing the dye molecules, both the systems would have yielded same or similar $I_{SC}$ values. In core−shell systems with another dye in the shell, photovoltaic characteristics with CdSe and ZnS nanoparticles in the core have been compared in Figure S5 in the Supporting Information; $I_{SC}$ in the former has been more than 10 times higher substantiating the role of CdSe nanoparticles in the photoinduced electron-transfer process followed by current in the external circuit. We have also studied a couple of systems with other dyes, which do not facilitate electron-transfer from CdSe nanoparticles. Such systems did not lead to an increase in $I_{SC}$ with dye adsorption. The results are in concurrence to our thesis that photoinduced electron-transfer from CdSe nanoparticles to RB molecules is responsible in yielding photocurrent in the external circuit.

**Systems with CdSe:RB: Variation of Different Parameters.** To establish electron-transfer from CdSe to RB molecules as the key process in obtaining photovoltaic characteristics, we have varied concentration of RB molecules on the shell of CdSe nanoparticles in the devices. That is, we linked RB molecules to CdSe nanoparticles for different length of time and fabricated devices based on such hybrid core−shell nanoparticles. Such devices actually compare systems with the same CdSe content but with different amount of RB molecules. Figure 5a shows that while the device without RB yields a low $I_{SC}$, the devices with increasing concentration of RB result an increased $I_{SC}$ with a saturation at 40% of RB on the shell of CdSe.

Devices were fabricated also with varied CdSe:RB concentration in P3HT matrix. Here we kept the extent of dye adsorption on the shell on CdSe nanoparticles the same (40%). It has been observed that the $I_{SC}$ was the highest when weight ratio between P3HT and CdSe:RB is 1:1 (Figure 5b). The $I_{SC}$ decreased when concentration of CdSe:RB in P3HT was changed to either directions. Since channels for transport of holes and electrons to the opposite electrodes are necessary to obtain photocurrent, the results in Figure 5b shows that once photoinduced electron-transfer from CdSe to RB occurs, channels for hole-transport (through P3HT) and electron-transport (through RB) remained equally important to generate $I_{SC}$. In other words, an increase in the concentration of CdSe:RB leads to fewer hole-transporting channels; similarly, a decrease in CdSe:RB concentration leaves the electrons confined leading to low $I_{SC}$.

**Photoaction Spectrum, $I_{SC}$ versus Light Intensity.** External quantum efficiency (EQE) of the devices with and

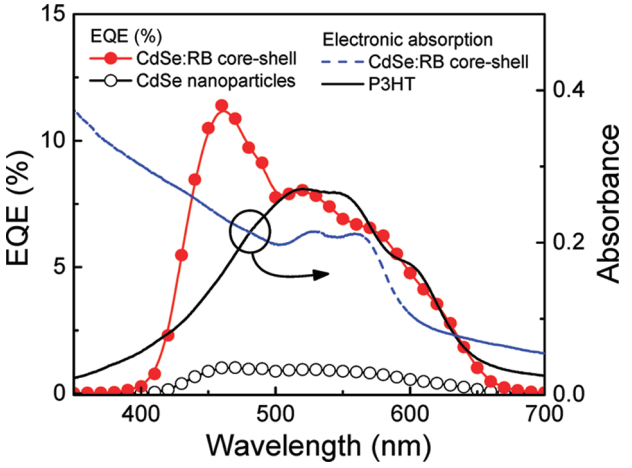


**Figure 6.** External quantum efficiency (EQE) spectrum of an ITO/PEDOT:PSS/P3HT:(CdSe:RB)/Al device with 40% RB on CdSe and ITO/PEDOT:PSS/P3HT:CdSe/Al device with weight ratio between P3HT and the nanoparticles being 1:1 in both the cases. Electronic absorption spectra of P3HT and CdSe:RB films on quartz are shown in the right axis.

without RB on CdSe are presented in Figure 6. The plots show a large enhancement in EQE (from 1 to 11%) at 470 nm with the incorporation of RB on CdSe nanoparticles. While all other components of the devices remain the same, the results again highlight the importance of photoinduced electron-transfer from CdSe to RB in obtaining high photovoltaic efficiency.

It may be mentioned here that the observed $I_{SC}$, $\eta$, and EQE in our P3HT:CdSe system are about one order lower than the reported values. Lower output in our devices could be due to our inability to complete device fabrication and characterization processes in inert environment. Still, when we compare our results in devices with and without RB, that is P3HT:(CdSe:RB) and P3HT:CdSe, we find a more than 10-fold enhancement in $I_{SC}$, $\eta$, and EQE in the former system due to electron-transfer from CdSe to RB. Hence, if we could have carried out the fabrication and characterization processes in inert environment, the respective values would have definitely exceeded the values reported in this work. Our results, at the least, highlight the importance of electron-transfer from the core to the shell of hybrid core−shell nanoparticles in photovoltaic devices.

The fact that the excitons generated at the CdSe nanoparticles followed by electron-transfers in fact yielded $I_{SC}$ in the photovoltaic solar cells can be understood from the spectral response of EQE of the devices. In Figure 6, we compare spectral response of EQE (photoaction spectrum) of a device based on CdSe:RB hybrid core−shell nanoparticles in the P3HT matrix with the electronic absorption spectra of P3HT and CdSe:RB films. This helps to find out the component of the device at which photogenerated excitons dissociate to lead to photocurrent. In the absorption spectrum of CdSe:RB films, while the band at 562 nm arises due to RB molecules, the band at 528 nm along with a continuum in the low wavelength region appear due to CdSe nanoparticles. P3HT films have showed a clear band with a peak at 520 nm. It may be noted that the absorption spectra were recorded in thin-films deposited on quartz; the devices whose photoaction spectra are presented in the figure are, on the other hand, fabricated on ITO-coated glass substrates. Hence, the photoaction spectrum in the range below 400 nm cannot be compared with electronic absorption spectra of the components. The results above 400 nm show that the photoaction spectrum of the devices with CdSe:RB nanoparticles in P3HT matrix resembles closely to the electronic absorption spectrum of CdSe:RB hybrid core−shell thin films. This shows that the photocurrent has yielded due to excitons formed mostly at CdSe nanoparticles. This further evidenced the fact that photoinduced electron-transfer from CdSe to RB has prompted photocurrent and photovoltaic effects in these devices based on hybrid core−shell nanoparticles.

We have compared the EQE spectrum of devices based on CdSe:RB and ZnS:RB core−shell nanoparticles (Figure S8a in the Supporting Information). As expected from the low $I_{SC}$ in the latter device, the overall EQE in the ZnS:RB system has been much lower than that in CdSe:RB-based devices. Additionally, the spectral response of EQE is different in the two systems evidencing the light-harvesting role of the nanoparticles. With another dye in the shell, the magnitude and spectral response of the EQE of devices based on CdSe and ZnS nanoparticles in the core differed in a similar fashion (Figure S8b in the Supporting Information), further substantiation of the role of the nanoparticles in light-harvesting and charge-generation processes.

It is customary to study illumination intensity dependence of $I_{SC}$ to rule out any heating effect in the observed photovoltaic characteristics. We have recorded $I-V$ characteristics of a device based on CdSe:RB core−shell nanoparticles in P3HT matrix under varied illumination intensities. As expected, the $I_{SC}$ increased with light intensity (Figure S9). The dependence has been linear with a slope of unity. The results, apart from ruling out any heating effect, show that the photovoltaic effect has been linear in the range of illumination intensities of our measurements.

## 4. Conclusion

In conclusion, we have formed hybrid core−shell nanoparticles based on CdSe nanoparticles in the core and dye molecules in the shell. These hybrid core−shell nanoparticles show photoinduced electron-transfer from the core to the shell. Such electron-transfers have been established from the quenching of PL spectrum and decrease in fluorescence lifetime of the nanoparticles. We have shown that photoinduced electron-transfer in a hybrid core−shell nanoparticle can be favorably used to obtain photocurrent for photovoltaic solar-cell applications. Devices with the core−shell nanoparticles in a P3HT matrix that also acts as a hole-transporting layer have exhibited a photovoltaic effect. By optimizing the concentration of electron acceptor and weight ratio of the nanoparticles in the P3HT matrix, we could obtain a photovoltaic device that has yielded a more than 10-fold

increase in short-circuit current, power conversion efficiency, and external quantum efficiency, as compared to the devices without the electron acceptor. The results, along with control experiments with ZnS nanoparticles in the core, show that light-harvesting in CdSe nanoparticles followed by charge separation in hybrid core−shell nanoparticles is an efficient method for solar cell applications.

**Acknowledgment.** This work is supported by Ramanna Fellowship SR/S2/RFCMP-02/2005. A.G. and A.K.R. acknowledge CSIR Junior Research Fellowship Nos. 09/080(0613)/2008-EMR-I (Roll No. 507076) and 09/080(0505)/2006-EMR-I (Roll No. 503974), respectively. The authors thank Santanu Jana for his assistance in synthesis of CdSe nanoparticles.

**Supporting Information Available:** Electronic absorption and photoluminescence spectra of CdSe:PB, CdSe:TBrPh, and ZnS:RB core−shells in dispersed solution at different times after adding the dye solution in CdSe dispersed solution from the top along with their components, fluorescence decay profile of PL emission of ZnS without and with RB in the shell, current−voltage characteristics of a device based on CdSe:TBrPh core−shell nanoparticles under dark and illumination conditions, a comparison of EQE in devices with CdSe and ZnS in the core and RB and TBrPh in the shell, and a plot of $I_{SC}$ versus light intensity. This material is available free of charge via the Internet at http://pubs.acs.org.